UDK 536.6:621.9.025.6:669.26
Original scientific article/Izvirni znanstveni članek

ISSN 1580-2949
MTAEC9, 57(4)325(2023)

INFLUENCE OF THE THERMAL CONDITION OF STEEL ON THE TRANSFORMATION TEMPERATURES OF TWO CHROMIUM HOT-WORK TOOL STEELS

VPLIV TOPLOTNEGA STANJA JEKLA NA PREMENSKE TEMPERATURE DVEH KROMOVIH ORODNIH JEKEL ZA DELO V VROČEM

Tilen Balaško*, Jožef Medved

Faculty of natural sciences and engineering, University of Ljubljana, Aškerčeva cesta 12, 1000 Ljubljana, Slovenia

Prejem rokopisa – received: 2023-03-07; sprejem za objavo – accepted for publication: 2023-05-18

doi:10.17222/mit.2023.822

The influence of the thermal condition of the steel on the transformation temperatures of two chromium hot-work tool steels was investigated. The steels studied were in two different thermal states: the soft -annealed state and the hardened-and-tempered state. The soft-annealed condition, i.e., the fully annealed condition, is a thermal state of steels in which the matrix is ferritic, and the carbon is chemically bonded in spherical carbides. The hardened-and-tempered condition, on the other hand, means a fully hardened-and-tempered martensitic matrix with uniformly distributed (primary and secondary) carbides. The samples were analysed in a simultaneous thermal analyser (STA) using the differential scanning calorimetry (DSC) method to determine the transformation temperatures. We also performed calculations based on the CALPHAD method to obtain the equilibrium temperatures of the transformations. The aim of the study was to determine the influence of different thermal conditions of chromium hot-work tool steels on the transformation temperatures such as solidus/liquidus temperatures, eutectoid transformation temperatures (A_1 and A_3), austenite solidification temperature and martensite transformation start temperatures. Since DSC analysis also measures thermal influence, we were able to determine the energies absorbed during eutectoid transformation and melting (endothermic processes) and the energies released during the solidification of δ-ferrite and austenite (exothermic processes), as well as the energies released during martensite transformation. It was found that hardening and tempering reduce both eutectoid transformation temperatures and that the solidification intervals are closer to those calculated. From an energetic point of view, hardening and tempering reduce the energies absorbed during melting.

Keywords: thermal analysis, chromium hot-work tool steels, differential scanning calorimetry, heat treatment

Avtorji so raziskovali vpliv toplotne obdelave (toplotnega stanja) jekla na premenske temperature dveh kromovih orodnih jekel za delo v vročem. Preiskovani jekli sta bili v dveh različnih toplotnih stanjih: mehko žarjenem in poboljšanem (kaljenje in popuščanje). Mehko žarjeno stanje, tj. popolnoma žarjeno stanje, je toplotno stanje jekel, kjer imamo feritno matrico, ogljik pa je kemično vezan v karbide krogline oblike. Po drugi strani pa kaljeno in popuščeno stanje pomeni popolnoma utrjeno in popuščeno martenzitno matrico z enakomerno porazdeljenimi (primarni in sekundarni) karbidi. Vzorce so avtorji preučevali v napravi za simultano termično analizo (STA) z metodo diferenčne vrstične kalorimetrije (DSC) za določitev premenskih temperatur. Naredili so tudi termodinamične izračune na podlagi metode CALPHAD za določanje ravnotežnih premenskih temperatur. Namen raziskave je bil ugotoviti vpliv različnih toplotnih stanj kromovih orodnih jekel za delo v vročem na premenske temperature, kot so solidus/likvidus, temperature evtektoidne transformacije (A_1 in A_3), začetne temperature strjevanja avstenita in temperature začetka martenzitne transformacije. Ker analiza DSC meri tudi toplotne učinke, so avtorji določili tudi energije, porabljene med evtektoidno transformacijo in taljenjem (endotermni procesi) in sproščene energije (eksotermni procesi) med strjevanjem δ-ferita, austenita in energije, sproščene med martenzitno transformacijo. Ugotovljeno je bilo, da poboljšano stanje zniža obe temperaturi evtektoidne transformacije in da so intervali strjevanja bližje tistim, ki so bili ravnotežno izračunani. Poboljšano stanje prav tako zmanjša energijo, absorbirano med taljenjem.

Ključne besede: termična analiza, kromova orodna jekla za delo v vročem, diferenčna vrstična kalorimetrija, toplotna obdelava

1 INTRODUCTION

Tool steels have high hardness, good wear resistance, resistance to deformation and breakdown, and increased durability at elevated temperatures.[1–7] According to the AISI classification, they can be divided into nine groups, with each group having a different designation.[1,7] Hot-work tool steels have the designation H and are normally used at higher temperatures and are divided into three groups: chromium, tungsten and molybdenum steels.[1,7] They are resistant to softening at elevated temperatures, even when exposed to them for prolonged periods of time and/or cyclic temperature loads.[1–5] Group-H steels are mainly used for the production of tools for the die-casting of light metals, the extrusion of polymers, forging, etc.[1–5,8]

It is well known that heat-treatment processes are unavoidable in hot-work tool steels. Normally, the heat treatment of hot-work tool steels is divided into two parts: (1) the heat treatment during the manufacturing process and (2) the final heat treatment that is usually carried out after machining.[3] From the end-user's point of view, the (2) final heat treatment is the most critical, since proper control of the final heat-treatment process

*Corresponding author's e-mail:
tilen.balasko@ntf.uni-lj.si

Table 1: Chemical composition of the hot-work tool steels examined, given in percent by weight

Sample	C	Si	Mn	P	S	Cr	Ni	Mo	V	W	Fe
Dievar	0.34	0.17	0.44	0.008	0.001	5.05	0.19	2.37	0.54	/	Bal.
H11	0.36	0.97	0.54	0.015	0.002	5.05	0.09	1.22	0.38	/	Bal.

ensures the achievement of the intended final microstructural constituents reflected in the desired mechanical properties. There are three important steps in the final heat-treatment process: austenitising, quenching (hardening) and tempering. Temperatures, soaking/tempering times and cooling rates are the main parameters we need to consider to achieve the desired mechanical properties.[1,3,6,7,9–11] This, together with the chemical composition, is the main reason why hot-work tool steels are resistant to softening at elevated temperatures.[1,3,4,6,9] There are several studies on the influence of elevated temperatures on the properties of hot-work tool steels[12–18] and studies on the influence of heat treatment on microstructure and mechanical properties.[19–25] On the other hand, to the best of our knowledge, there are no studies on the influence of heat treatment on transformation temperatures such as A_1, A_3, M_S, B_S, T_L, T_S, the solidification onset temperature of austenite, the solidification interval and the energies absorbed/released during the heating and cooling of hot-work tool steel. These temperatures, especially the eutectoid reaction temperatures, are important for the use of hot-work tool steels. This is because the closer the operating temperature is to the temperature of the start of the eutectoid reaction (A_1), the faster the steel will soften when used at elevated temperatures. Normally, these temperatures are determined by hardening the steel at austenitisation temperatures where the microstructure consists of austenite.

So, our question was, how do these temperatures change for steel in the hardened-and-tempered condition compared to those in the soft-annealed condition? Because normally steels are used in the hardened-and-tempered condition. And how does this affect the energies absorbed and released during heating or cooling? The topic is also interesting from the point of view of the 3D printing or additive manufacturing of tool steels, both in terms of energies and transformation temperatures. Differential scanning calorimetry (DSC) was performed to determine the effects of heat treatment on the transformation temperatures and the energies absorbed or released during heating and cooling. Two different chromium hot-work tool steels were investigated in two thermal states. The first was the soft-annealed condition, which we used as a reference since tool steels are usually supplied in the "as-delivered" condition, i.e., in the fully annealed condition in which the matrix is ferritic and the carbon is chemically bonded in spherical carbides.[7] The second thermal condition was the hardened and tempered, i.e. fully hardened-and-tempered martensitic matrix with uniformly distributed (primary and secondary) carbides.[7]

2 EXPERIMENTAL PART

Two chromium hot-work tool steels with the chemical composition given in **Table 1**, measured by wet chemical analysis and infrared absorption after combustion with ELTRA CS-800, were investigated.

At the beginning, the investigated steels were heat treated. The heat-treatment processes used are listed in **Table 2** and the soaking time was 30 minutes in all cases. Hardening was carried out in oil, followed by tempering in the Bosio EUP-K 6/1200 chamber furnace. The tempering time was 2 hours for all individual tempering stages and steels examined. As an atmosphere of air was used, 2 mm of the steel surface was milled off due to decarburisation and oxidation during heat treatment.

Table 2: Heat treatment processes for steels

Sample	Hardness (HRC)	Austenitization temperature (°C)	First tempering (°C)	Second tempering (°C)
Dievar	42–44	1025	550	630
H11	42–44	1020	550	620

To ensure that the heat treatment was successful, we measured the Vickers hardness with an Instron Tukon 2100B. The average values of the measurements can be found in **Table 3**. We do not include these values in the results because we only wanted to check that the heat treatment was successful and to ensure that the steels studied were in two different thermal conditions. Since the steels studied are in two different states, i.e., soft-annealed and hardened-and-tempered, the first ones were named Dievar and H11 (soft annealed) and the second ones DievarHT and H11HT (hardened and tempered).

Table 3: Measured hardness of the samples

Sample	Hardness/HV 10
Dievar	198
DievarHT	440
H11	180
H11HT	478

Since the microstructures of all the steels examined have already been analysed in both thermal states, we have not carried out any further metallographic analysis. It is known that the microstructure of hot-work tool steels in the soft-annealed condition consists of a ferritic matrix and carbon chemically bonded in spherical carbides.[7] The hardened-and-tempered microstructure, on the other hand, consists of a martensitic matrix with uniformly distributed (primary and secondary) carbides.[7] In

Dievar steels, the hardened-and-tempered microstructure consists of a martensitic matrix, $M_{23}C_6$ ($(Cr,Mo,Fe)_{23}C_6$), M_6C ($(Mo,Fe,V)_6C$) and M_2C ($(Mo,V,Cr)_2C$) plus small amounts of VC and Ti(CN).[26,27] The microstructure of H11 steel consists of a martensitic matrix, $M_{23}C_6$ ($(Cr,Mo,Fe)_{23}C_6$), small amounts of VC and Ti(CN).[27,28]

After heat treatment, the samples for DSC analysis with dimensions h = 4 mm and Φ = 4 mm were prepared. The DSC analysis was carried out with a NETZSCH STA (Simultaneous Thermal Analyzer) Jupiter 449C.

First, CALPHAD (CALculation of PHAse Diagrams) simulations were performed with Thermo-Calc 2023a software using the TCFE10 (TCS Steel and Fe-alloys Database) thermodynamic database. The calculations resulted in equilibrium transformation temperatures for all steels investigated.

DSC analysis was performed in the NETZSCH STA Jupiter 449C instrument, using a protective Ar5.0 atmosphere with a flow rate of 30 mL·min^{-1} throughout the experiment. The temperature programme was the same for all steels studied, heating and cooling rates were 10 °C min^{-1}, samples were heated from room temperature to 1550 °C and then cooled to room temperature. Empty Al_2O_3 crucibles were used as a reference and the masses of the samples varied between 390 mg and 410 mg. The DSC heating and cooling curves were used to determine the experimental transformation temperatures of the steels studied. The analysis is well known and is often used to determine the transformation temperatures of metal alloys.[29–33]

3 RESULTS AND DISCUSSION

Since the steels studied are in two different states, i.e., soft annealed and hardened and tempered, the first were named Dievar and H11 (soft annealed) and the second DievarHT and H11HT (hardened and tempered). To avoid confusion and errors, we refer to the soft-annealed thermal state as this is the thermal state in which hot-work tool steels are normally supplied by the manufacturer. Heat treatment refers to the hardened-and-tempered condition, as hardening and tempering of the steel in the soft-annealed condition is usually carried out before hot work steels are used, to obtain the specified mechanical and other properties.

3.1 CALPHAD calculations

Calculations were carried out to determine the equilibrium transformation temperatures for the steels studied. The focus was on the eutectoid transformation temperatures, the liquidus, solidus and austenite solidification onset temperatures.

The two calculated equilibrium diagrams are shown in the following figures. These are so-called "property diagrams", which show the amount of thermodynamically stable equilibrium phases as a function of temperature. The diagrams shown (**Figure 1**) were calculated

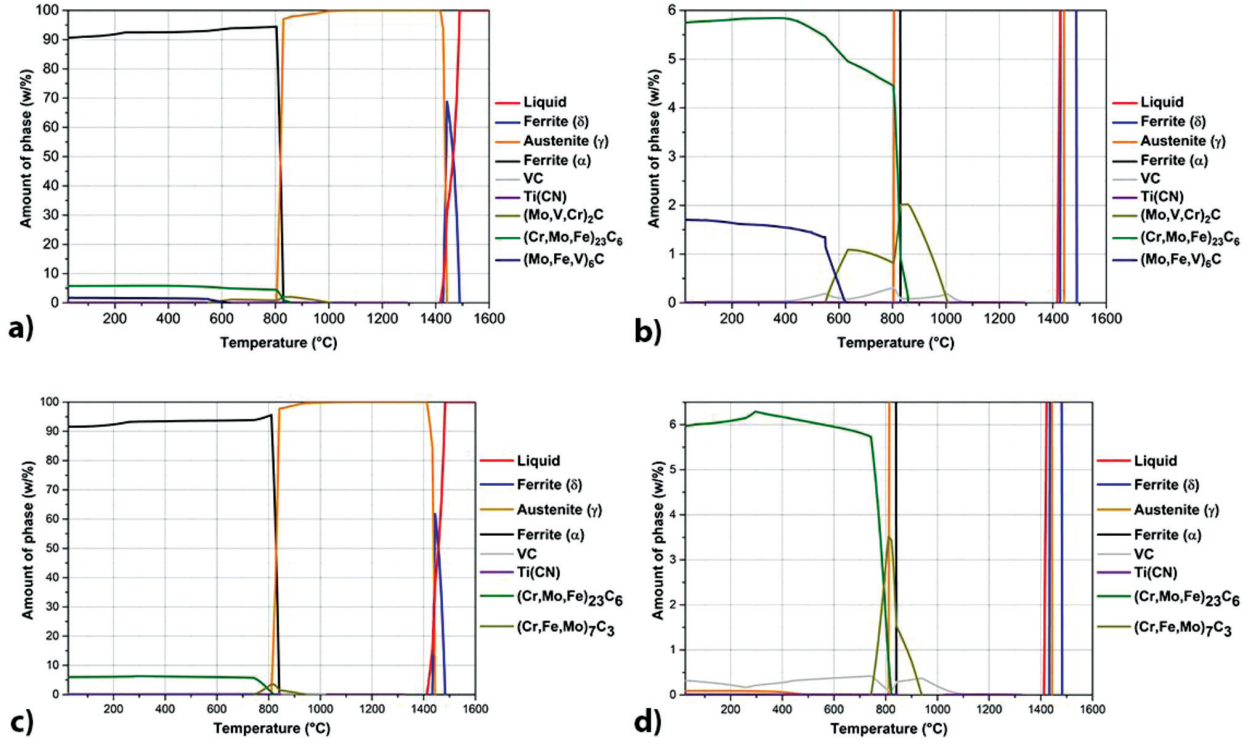

Figure 1: Amount of all thermodynamically stable equilibrium phases as a function of temperature: a) and b) for Dievar steel and c) and d) for H11 steel

based on the chemical composition of the steels Dievar and H11. From the data calculated for the above diagrams, we have determined the transformation temperatures for the steels studied and compiled them in a table (**Tables 4 and 5**).

If we first look at the solidification interval (**Table 4**), there are no major differences. The closest solidification interval is that of H11 steel, followed by Dievar. The differences between these two are minimal, which was to be expected as the chemical composition is very similar.

Table 4: Transformation temperatures of the investigated steels, calculated with the CALPHAD method

Sample	Liquidus (°C)	Austenite (°C)	Solidus (°C)	Solidification interval (°C)
Dievar	1491	1443	1418	73
H11	1484	1444	1414	70

The eutectoid transformation temperatures (**Table 5**) are also very similar, which consequently also applies to the two-phase field intervals.

Table 5: Equilibrium temperatures of the eutectoid transformation of the steels examined, calculated with the CALPHAD method

Sample	Ae_1 (°C)	Ae_3 (°C)	Two-phase field interval (°C)
Dievar	808	832	24
H11	814	843	29

3.2 DSC analysis

In the following we have summarised the results of the DSC analysis in tables and the diagrams of the heating and cooling curves of all the samples examined are also shown. First, the DSC heating curves are shown (**Figure 2**), from which we can determine the solidus temperature, the eutectoid transformation temperatures (Ac_1 and Ac_1), the Curie point and the energies absorbed during eutectoid transformation and melting (endothermic processes). On the other hand, from the DSC curves during cooling (**Figure 3**) we can determine the liquidus temperature, the starting temperature of austenite solidification and the starting temperatures of martensite transformation. Under the aspect of energies, we can determine the released energies (exothermic processes) during the solidification of δ-ferrite, austenite and the released energies during the martensite transformation.

The results are discussed selectively by steel type and at the end a comparison of the results is made and discussed. At this point we must add that we were also able to determine the Curie temperature from the DSC heating curves (**Figure 2**). There were slight changes in Curie temperatures between the samples in the hardened-and-tempered condition and in the soft-annealed condition. For Dievar steel it was 766.4 °C and 771.4 °C for the hardened-and-tempered and soft-annealed samples, respectively. For H11 steel the trend was almost the same: the temperature was 758.4 °C and 759.8 °C for the hardened-and-tempered and soft-annealed samples, respectively.

First, we will discuss the influence of heat treatment on the DSC heating curves (**Figure 2**), from which we can determine the solidus temperature, the eutectoid transformation temperatures (Ac_1 and Ac_1), the Curie point and the energies absorbed during eutectoid transformation and melting (endothermic processes). The results of the DSC heating curves are summarised in **Table 6** and **Table 7**.

The next results (**Table 6**) refer to the eutectoid transformation temperatures and are discussed selectively by steel grade, starting with Dievar steel, where both temperatures (Ac_1 and Ac_3) are lower in the case of the hardened-and-tempered sample. Consequently, the interval of the two-phase field is 4.8 °C smaller for the hardened-and-tempered sample. The same trend continues for H11 steel, where both temperatures (Ac_1 and Ac_3) are lower in the case of the hardened-and-tempered sample, but the interval of the two-phase field remains almost the same, the difference being only 0.3 °C.

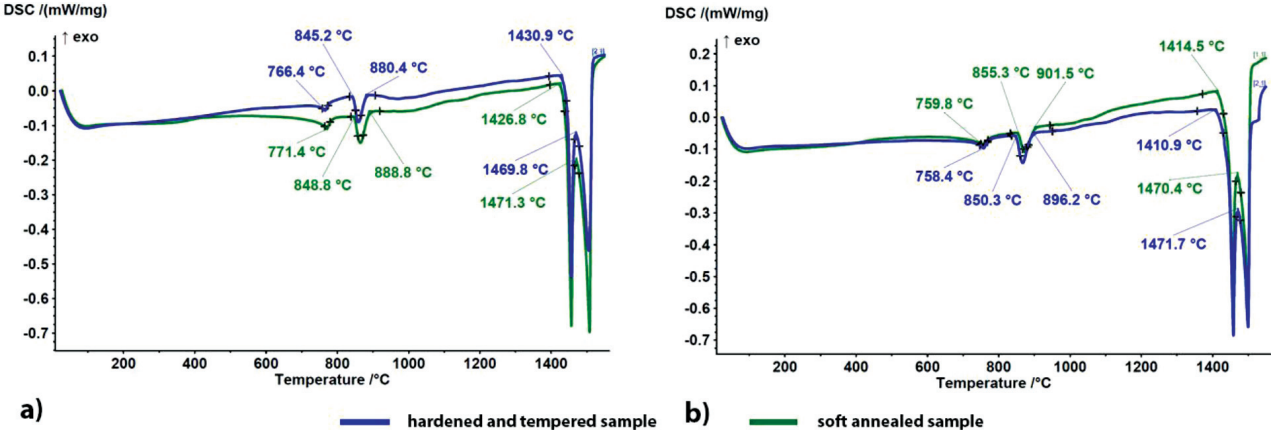

Figure 2: Heating DSC curves of the investigated samples: a) Dievar and b) H11

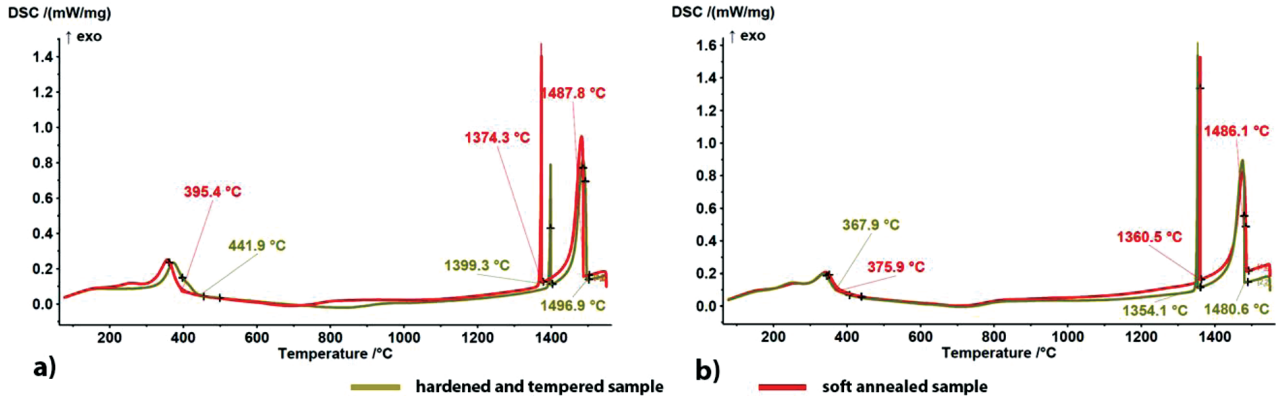

Figure 3: Cooling DSC curves of the investigated samples: a) Dievar and b) H11

In summary, hardening and tempering lowers both eutectoid transformation temperatures (Ac_1 and Ac_3), but the interval of the two-phase field remains almost the same as for the soft-annealed samples.

Table 6: Eutectoid transformation temperatures of the investigated samples, with corresponding two-phase field interval

Sample	Ac_1/°C	Ac_3/°C	Two-phase field interval/°C
Dievar	848.8	888.8	40.0
DievarHT	845.2	880.4	35.2
H11	855.3	901.5	46.2
H11HT	850.3	896.2	45.9

The following table (**Table 7**) compiles the energies absorbed during eutectoid transformation and melting. It is obvious that in the case of Dievar steel, the sample in the hardened-and-tempered state absorbed less energy during the eutectoid transformation and melting. The same trend continues for H11 steel, where the absorbed energy during melting is lower for the sample in the hardened-and-tempered state. However, there is a difference in H11 steel: the energy absorbed during the eutectoid transformation is higher for the sample in the hardened-and-tempered state. The main reason for this is the microstructure, i.e., the final hardness after tempering, which was higher (478 HV10) than for Dievar steel (440 HV10). This means that even more alloying elements were dissolved in the martensitic matrix, which was also not sufficiently tempered and consequently more energy was needed for the eutectoid transformation than for the Dievar steel in the hardened-and-tempered state with lower hardness after tempering.

From the results obtained, it appears that hardened-and-tempered samples absorb less energy during melting than samples in the soft-annealed condition. This is somehow to be expected as the martensitic matrix is metastable from a thermodynamic point of view compared to the ferritic matrix, more alloying elements are dissolved in the matrix and the carbides are small and homogeneously distributed in the sample. In contrast, the samples in the soft-annealed condition have a thermodynamically stable ferritic matrix with large spherical carbides that are inhomogeneously distributed. There were also no major differences in the thermal state of the samples with regard to energy absorption during the eutectoid transformation.

Table 7: Absorbed energies during eutectoid transformation and melting (endothermic processes) of the investigated samples

Sample	Energies/J·g^{-1}	
	Eutectoid transformation	Melting
Dievar	–11.410	–194.0
DievarHT	–9.388	–147.2
H11	–11.110	–184.6
H11HT	–13.640	–165.2

Next, we discuss the influence of heat treatment on solidification, i.e., the cooling DSC curves (**Figure 3**), from which we can determine the liquidus temperature, the starting temperature of austenite solidification and the starting temperatures of martensite transformation. From the aspect of energies we can determine the released energies (exothermic processes) during the solidification of δ-ferrite, austenite and the released energies during the martensite transformation. The results of the DSC curves during cooling are summarised in **Tables 8–10**.

In the case of the Dievar steel the samples in the hardened-and-tempered condition have higher liquidus, solidus and austenite solidification temperatures (**Table 8**). Consequently, the solidification interval is also extended, but only by 5 °C. For H11 steel the tendency is different, there are smaller differences in the liquidus and austenite solidification temperatures than for Dievar steel. On the other hand, the differences in solidus temperatures are almost the same compared to Dievar steel. In this case the solidification interval for steels in both thermal states remains almost the same: the difference is only 1.9 °C. The reason for this is probably the hardness of the hardened-and-tempered sample, which is higher than for the Dievar steel.

Table 8: Liquidus, solidus and austenite solidification temperatures, with corresponding solidification interval of the investigated samples

Sample	Liquidus/°C	Austenite/°C	Solidus/°C	Solidification interval/°C
Dievar	1487.8	1374.3	1426.8	61.0
DievarHT	1496.9	1399.3	1430.9	66.0
H11	1486.1	1360.5	1414.5	71.6
H11HT	1480.6	1354.1	1410.9	69.7

Table 9: Released energies during solidification and martensite transformation (exothermic processes) of the investigated samples

Sample	Energies/J·g^{-1}			
	δ-ferrite solidification	Austenite solidification	Entire solidification (δ-ferrite and austenite)	Martensite transformation
Dievar	119.60	17.47	137.07	45.84
DievarHT	109.40	10.60	120.00	55.25
H11	110.40	16.45	126.85	30.18
H11HT	124.30	18.38	142.68	23.89

The results show that the liquidus, solidus and austenite solidification temperatures hardly differ, which means that the solidification interval also remains almost the same.

We continue with the results concerning the released energies (exothermic processes) obtained when cooling the samples (**Table 9**). The samples of Dievar steel in the hardened-and-tempered condition released less energy during solidification than the soft-annealed samples. Only the energy released during the martensite transformation was higher. Interestingly, the opposite is true for the H11 steel: the hardened-and-tempered samples released more energy during solidification than the soft-annealed samples and less energy during martensite transformation.

Overall, the energy released during solidification is lower for the Dievar steel in the hardened-and-tempered condition than for the samples in the soft-annealed condition. The deviation concerns steel H11, where more energy was released during solidification of the hardened-and-tempered sample. This is related to the solidification interval, which remains almost unchanged in the case of steel H11 (**Table 8**).

At the end of the cooling another peak could be analysed on the DSC curves, which belonged to the martensite transformation (**Figure 3** and **Table 10**). For Dievar steel, the starting temperature of martensite transformation was higher for the sample in the hardened-and-tempered condition than for the sample in the soft-annealed condition, the difference being 46.5 °C. However, this was reversed for H11 steel, i.e., the martensite transformation temperature was lower for the sample in the hardened-and-tempered condition than for the sample in the soft-annealed condition, but the difference was only 8 °C. The reasons for this are the same as before (the higher hardness of the hardened-and-tempered samples resulting in a less-tempered martensitic matrix, more alloying elements dissolved in the matrix, etc.). The other reason that also needs to be considered is the interval of the two-phase field (between A_1 and A_3), and the results show that the H11 steel has almost the same interval in both cases (**Table 10**).

Table 10: Starting temperatures of the martensite transformation of the investigated samples

Sample	M_S/°C
Dievar	395.4
DievarHT	441.9
H11	375.9
H11HT	367.9

Overall, we were able to determine the Curie temperatures from DSC heating curves for both steels studied. The eutectoid transformation temperatures (Ac_1 and Ac_3) are the next temperatures to be considered. Overall, it can be seen that hardening and tempering lower both eutectoid transformation temperatures. However, the interval of the two-phase field remains almost the same as for the samples that are in the soft-annealed state. If we consider the absorbed energies during eutectoid transformation and melting (endothermic processes). It seems that hardening and tempering reduce the energies absorbed during the eutectoid transformation. The results of the H11 steel stand out, the reasons being the same as before. The alternative results of energies absorbed during melting were consistent for all the samples studied. Hardening and tempering lowers the energy absorbed during melting in all cases. This is to be expected to some extent as the martensitic matrix of the hardened-and-tempered samples is metastable, has more alloying elements dissolved and there are mainly fine and small carbides homogeneously distributed in the sample. In the soft-annealed samples, on the other hand, there is a stable ferritic matrix with large spherical carbides that are not homogeneously distributed, and in general the microstructure is closer to equilibrium than in the hardened-and-tempered samples.

Based on the solidification (DSC cooling curves) we can assume that there are minor differences between the

liquidus and solidus temperatures. The solidification interval also remains almost the same for both thermal states, which means that there are no major influences of the heat treatment on the solidification of the steels studied. As far as the energies released during solidification are concerned, the energies in the Dievar steels are lower in the hardened-and-tempered samples than in the soft-annealed samples. However, this is reversed for the H11 steel, as the hardness of the hardened-and-tempered samples was higher than for the Dievar steel. This means that the samples were not sufficiently tempered compared to the others and even more alloying elements were dissolved in the martensitic matrix. This results in more energy being released during the solidification of a hardened-and-tempered sample than a soft-annealed sample. There is no trend in terms of energies released during martensite transformation and no general observations can be made. Only one other thing can be explained from the DSC cooling curves, and that is the starting temperatures of martensite transformation. The martensite transformation temperature is higher for Dievar steel in the hardened-and-tempered condition. However, the results for H11 steel differ from this, as explained earlier.

A final point to analyse is the comparison of the calculated equilibrium transformation temperatures with the experimental temperatures obtained by DSC analysis. As far as the austenite solidification temperatures are concerned, the calculated temperatures were closer to those of the soft-annealed samples in the case of the Dievar steel and closer to those of the hardened-and-tempered samples in the case of the H11 steel. However, if we consider the solidification interval, there is a tendency for the results of the hardened-and-tempered samples to be closer to the calculated values for all the steels studied.

4 CONCLUSIONS

In summary, then, we can write the following:

- Chromium hot-work tool steels hardly differ in terms of liquidus and solidus temperatures. The solidification interval remains also almost the same for both thermal states, which means that there are no major influences of heat treatment on the solidification of chromium hot-work tool steels;
- we were able to determine the Curie temperatures, which were lower for hardened-and-tempered samples;
- hardening and tempering reduce both the energy absorbed in the eutectoid transformation and in the melting;
- we could determine the starting temperature of the martensitic transformation, hardening and tempering reduce both eutectoid transformation temperatures. However, the interval of the two-phase field remains almost the same as for the samples in the soft-annealed state;
- the calculated liquidus and solidus temperatures are closer to the temperatures determined for the soft-annealed samples;
- the solidification intervals of the hardened-and-tempered samples are closer to the calculated values.

5 REFERENCES

[1] G. Roberts, G. Krauss, R. Kennedy, Tool Steels: 5th ed., ASM International, Materials Park 1998, 364

[2] C. R. Sohar, Lifetime controlling defects in tool steels, Springer, Berlin 2011, 224

[3] R. A. Mesquita, Tool steels: properties and performance, CRC Press, Boca Raton 2016, 245

[4] ASM handbook, volume 1: Properties and selection: irons, steels, and high-performance alloys, ASM International, Materials Park 1990, 1063

[5] W. F. Hosford, Iron and Steel, Cambridge University Press, Cambridge 2012, 310

[6] Heat Treater's Guide: Practices and Procedures for Irons and Steels, ASM International, Metals Park 1995, 904

[7] C. Højerslev, Tool steels, Risø National Laboratory, Roskilde 2001, 25, http://orbit.dtu.dk/files/7728903/ris_r_1244.pdf, January 2021

[8] J. Sjöström, Chromium martensitic hot-work tool steels - damage, performance and microstructure, Doctoral thesis, Karlstad University, 2004, 53, http://www.diva-portal.org/smash/get/diva2:24899/FULLTEXT01.pdf, 21.01.2013

[9] G. Krauss, Steels: Processing, Structure, and Performance, ASM International, Materials Park 2015, 682

[10] G. E. Totten, Steel Heat Treatment: Metallurgy and Technologies, CRC Press, Boca Raton 2006, 848

[11] G. N. Haidemenopoulos, Physical Metallurgy: Principles and Design, CRC Press, Boca Raton 2018, 476

[12] Q. Zhou, X. Wu, N. Shi, J. Li, N. Min, Microstructure evolution and kinetic analysis of DM hot-work die steels during tempering, Mater. Sci. Eng. A, 528 (**2011**) 18, 5696–5700, doi:10.1016/j.msea.2011.04.024

[13] A. Medvedeva, J. Bergström, S. Gunnarsson, J. Andersson, High-temperature properties and microstructural stability of hot-work tool steels, Mater. Sci. Eng. A, 523 (**2009**) 1–2, 39–46, doi:10.1016/j.msea.2009.06.010

[14] Z. Zhang, D. Delagnes, G. Bernhart, Microstructure evolution of hot-work tool steels during tempering and definition of a kinetic law based on hardness measurements, Mater. Sci. Eng. A, 380 (**2004**) 1, 222–230, doi:10.1016/j.msea.2004.03.067

[15] N. Mebarki, D. Delagnes, P. Lamesle, F. Delmas, C. Levaillant, Relationship between microstructure and mechanical properties of a 5% Cr tempered martensitic tool steel, Mater. Sci. Eng. A, 387–389 (**2004**), 1-2, 171–175, doi:10.1016/j.msea.2004.02.073

[16] A. Jilg, T. Seifert, Temperature dependent cyclic mechanical properties of a hot work steel after time and temperature dependent softening, Mater. Sci. Eng. A, 721 (**2018**), 96–102, doi:10.1016/j.msea.2018.02.048

[17] D. Caliskanoglu, I. Siller, R. Ebner, H. Leitner, F. Jeglitsch, W. Waldhauser, Thermal Fatigue and Softening Behavior of Hot Work Tool Steels, Proc. 6th Int. Tool. Conf., Karlstad 2002, 707–719

[18] R. Markežič, N. Mole, I. Naglič, R. Šturm, Time and temperature dependent softening of H11 hot-work tool steel and definition of an anisothermal tempering kinetic model, Mater. Today Commun., 22 (**2020**), 1–7, doi:10.1016/j.mtcomm.2019.100744

[19] S. Kheirandish, H. Saghafian, J. Hedjazi, M. Momeni, Effect of heat treatment on microstructure of modified cast AISI D3 cold work tool steel, J. Iron Steel Res. Int., 17 (**2010**), 40–45, doi:10.1016/S1006-706X(10)60140-9

[20] C. J. Chen, K. Yan, L. Qin, M. Zhang, X. Wang, T. Zou, Z. Hu, Effect of Heat Treatment on Microstructure and Mechanical Properties

of Laser Additively Manufactured AISI H13 Tool Steel, J. Mater. Eng. Perform., 26 (**2017**) 11, 5577–5589, doi:10.1007/s11665-017-2992-0

[21] M. Priyadarshini, A. Behera, C. K. Biswas, D. K. Rajak, Experimental Analysis and Mechanical Characterization of AISI P20 Tool Steel Through Heat-Treatment Process, J. Bio- Tribo-Corrosion, 8 (**2022**) 1, 1–10, doi:10.1007/s40735-021-00607-3

[22] F. Huber, C. Bischof, O. Hentschel, J. Heberle, J. Zettl, K. Y. Nagulin, M. Schmidt, Laser beam melting and heat-treatment of 1.2343 (AISI H11) tool steel – microstructure and mechanical properties, Mater. Sci. Eng. A, 742 (**2018**), 109–115, doi:10.1016/j.msea.2018.11.001

[23] I. Souki, D. Delagnes, P. Lours, Influence of heat treatment on the fracture toughness and crack propagation in 5% Cr martensitic steel, Procedia Eng., 10 (**2011**), 631–637, doi:10.1016/j.proeng.2011.04.105

[24] N. B. Dhokey, S. S. Maske, P. Ghosh, Effect of tempering and cryogenic treatment on wear and mechanical properties of hot work tool steel (H13), Mater. Today Proc., 43 (**2021**), 3006–3013, doi:10.1016/j.matpr.2021.01.361

[25] W. R. Prudente, J. F. C. Lins, R. P. Siqueira, P. S. N. Mendes, R. E. Pereira, Microstructural evolution under tempering heat treatment in AISI H13 hot-work tool steel, Int. J. Eng. Res. Appl., 7 (**2017**) 4, 67–71, doi:10.9790/9622-0704046771

[26] T. Balaško, M. Vončina, J. Burja, J. Medved, Influence of Heat Treatment on the High-Temperature Oxidation Behaviour of Chromium-Molybdenum-Vanadium Alloyed Hot-Work Tool Steel, Mater. Tehnol., 56 (**2022**) 2, 233–241, doi:10.17222/mit.2022.406

[27] T. Balaško, M. Vončina, J. Medved, Simultaneous thermal analysis of the high-temperature oxidation behaviour of three hot-work tool steels, J. Therm. Anal. Calorim., 148 (**2022**), 1251–1264, doi:10.1007/s10973-022-11616-w

[28] T. Balaško, M. Vončina, J. Burja, B. Š. Batič, J. Medved, High-temperature oxidation behaviour of AISI H11 tool steel, Metals, 11 (**2021**) 5, doi:10.3390/met11050758

[29] E. Kaschnitz, P. Hofer-Hauser, W. Funk, Electrical resistivity measured by millisecond pulse-heating in comparison to thermal conductivity of the hot work tool steel AISI H11 (1.2343) at elevated temperature, High Temp. – High Press., 49 (**2020**) 1–2, 75–87, doi:10.32908/hthp.v49.825

[30] T. Balaško, J. Burja, J. Medved, Effect of Ni on solidification of duplex low-density steels, J. Therm. Anal. Calorim., 142 (**2020**) 5, 1605–1611, doi:10.1007/s10973-020-10254-4

[31] E. Wielgosz, T. Kargul, Differential scanning calorimetry study of peritectic steel grades, J. Therm. Anal. Calorim., 119 (**2015**) 3, 1547–1553, doi:10.1007/s10973-014-4302-5

[32] B. Smetana, M. Žaludová, S. Zlá, J. Dobrovská, M. Cagala, I. Szurman, D. Petlák, Application of high temperature DTA technique to Fe based systems, Proc. of the 19th Int. Metallurgical and Materials Conference, Roznov pod Radhostem 2010, 357–362

[33] B. Smetana, S. Zlá, J. Dobrovská, P. Kozelsky, Phase transformation temperatures of pure iron and low alloyed steels in the low temperature region using DTA, Int. J. Mater. Res., 101 (**2010**) 3, 398–408, doi:10.3139/146.110283